Eur. J. Mech., B/Fluids, **17,** n° 2, 165-185, 1998

Absolute instability conditions for variable density, swirling jet flows

D. W. LIM and L. G. REDEKOPP *

ABSTRACT. – Two different vortex sheet models are used to study the transition from absolute to convective instability in variable-density, swirling jet flows. It is found that swirl enhances the tendency for absolute instability in a jet issuing into a non-swirling medium when the vortical core of the swirling flow is small compared to the jet radius. When the size of the vortical core approximates the size of the jet, the effect of swirl on promoting absolute instability is quite weak. The trend toward absolute instability is accentuated when the jet is heated relative to the ambient. If the flow external to the jet also possesses swirl, the tendency toward absolute instability is increased when the jet shear layer is centrifugally unstable according to Rayleigh's criterion (*i.e.*, the circulation decreases with increasing radius) and is decreased when the shear layer is centrifugally stable. © Elsevier, Paris.

1. Introduction

The dynamics and mixing characteristics of jet flows have been studied quite extensively over a number of decades motivated, for example, by efforts to increase combustion efficiency or to decrease noise radiation. Advanced designs for combustors, quiet jet engines, and other technological applications, depend on the identification of strategies, either passive or active, for effectively modifying the spreading rate of shear layers formed at the exit of a jet. To this end, the study of the linear instability properties of various mean jet flow states has served as a useful guide in delineating the role of various control parameters in modifying jet entrainment and mixing. For example, instability calculations have provided a firm basis for understanding the role of the velocity ratio in the spreading of mixing layers, the observed reduction in the growth of compressible mixing layers as the convective Mach number is increased, and the enhanced entrainment of low-density jets compared to their constant density counterparts. Instability studies have also served to guide the formulation of both physical and numerical experiments related to this subject. A summary of some of the contributions of instability theory to our understanding of jet flows has been provided by Michalke (1984).

One particular class of jet flows, namely that of swirling jets, has received considerable attention in recent years. Swirl is naturally present in the exhaust from a turbine or an axial flow pump and may be deliberately generated in some cases to influence jet mixing through design of the jet nozzle. Experiments have revealed that low-speed, swirling jets can, under some conditions, realize higher spreading and entrainment rates than their non-swirling counterparts (e.g., Panda and McLaughlin, 1994). These results have spurred the formulation of several instability studies aimed at elucidating the competition of azimuthal and streamwise vorticity in determining the growth of either axisymmetric or helical disturbances in a circular jet. There are two basic types of inviscid instability which operate concurrently in swirling jets, the shear instability associated with the inflection point in the streamwise velocity profile and the centrifugal instability associated with the radial profile of swirl velocity (cf. Drazin and Reid, 1981). The focus of almost all instability studies related to swirling jet flows has been directed toward determining how the maximum temporal growth rate and the bandwidth of

* Department of Aerospace Engineering, University of Southern California, Los Angeles, California, 90089-1191, USA.

0997-7546/98/02/© Elsevier, Paris

unstable wavenumbers vary with swirl ratio, the ratio of the azimuthal circulation to the streamwise circulation of the base state flow field. However, understanding how either the temporal or spatial growth rates vary with swirl ratio, by itself, does not necessarily reveal how the spreading rate of the jet, or even the shear layers at the jet exit, will vary with this parameter. This statement is quite amply illustrated by the experimental findings of Panda and McLaughlin (1994). They report that the growth rate of disturbances seem to diminish as swirl is increased, yet they also show definitive increases in jet spreading rates with increasing swirl. If this behavior is to be understood from an instability point of view, other characteristics must exist which are of particular dynamical significance.

An important issue relating to the dynamics of disturbances is the propagative nature of the spectrum of unstable waves. The point of concern is not only the growth rate of a particular wave mode, but whether the local instability at any parameter condition is of absolute or convective type; that is, whether unstable waves can propagate both upstream and downstream or only in one direction. The answer to this question is pivotal to predicting the possible existence of a global instability, an instability which gives rise to robust, synchronous, spatio-temporal dynamics, or to assessing the potential for control disturbances injected at the jet origin to influence the spatial development of a jet through exploitation of the natural spatial amplifier of the jet wave guide (cf. Chomaz *et al.*, 1988, 1991; and Huerre and Monkewitz, 1990). Although it is only a conjecture at the present time, it is not unreasonable to think of the appearance of vortex breakdown in a developing swirl flow as the manifestation of the onset of a global instability. This connection was, in fact, the primary motivation for initiating this work.

The present work describes calculations of the absolute/convective nature of unstable disturbances for some simple models of a swirling jet. Although the flow configurations studied are comprised of layers having constant axial velocity and axial vorticity, the results are expected to provide a useful guide in determining the nature of any local instability in a variable-density swirling jet, and in estimating conditions under which the onset of a global dynamics might be possible. While this work was in progress, the authors learned of related studies with similar objectives (cf. Loiseleux *et al.*, 1997; Delbande *et al.*, 1997; and Billant *et al.*, 1997). Although the basic motivation of both efforts is similar, there is overlap on only one flow model, the Rankine vortex jet, and that for the case of a homogenous or uniform density flow. We include the important effect of variable density in the present work and analyze several different configurations of swirling flows to assess the role of the size of the vortical core of the swirling flow on the character of the linear instability of a jet.

2. Problem formulation

We consider the instability of a steady, parallel, rotationally-symmetric flow defined by the velocity field $\vec{V} = U(r)\hat{e}_x + V(r)\hat{e}_\theta$, where r is the radial coordinate in a cylindrical polar coordinate system with $\hat{e}_x$ in the axial direction and $\hat{e}_\theta$ in the azimuthal direction. The mean pressure field $P(r)$ associated with this flow field satisfies

$$\rho\frac{V^2}{r} = \frac{dP}{dr}. \tag{1}$$

The model swirling jet flows studied here are constructed by specifying different profiles of both the swirl velocity $V(r)$ and the axial velocity $U(r)$ in concentric cylindrical layers. Considering the fluid to be incompressible and inviscid, the linearized system of equations defining the perturbed velocity field

$\vec{q} = u\hat{e}_x + v\hat{e}_\theta + w\hat{e}_r$, relative to the mean velocity $\vec{V}(r)$, and the perturbed pressure field $p(x,\theta,r,t)$ in any layer is given by

$$\frac{\partial u}{\partial x} + \frac{1}{r}\frac{\partial v}{\partial \theta} + \frac{1}{r}\frac{\partial (rw)}{\partial r} = 0, \tag{2a}$$

$$\frac{\partial u}{\partial t} + U\frac{\partial u}{\partial x} + \frac{V}{r}\frac{\partial u}{\partial \theta} + wU' = -\frac{1}{\rho}\frac{\partial p}{\partial x}, \tag{2b}$$

$$\frac{\partial v}{\partial t} + U\frac{\partial v}{\partial x} + \frac{V}{r}\frac{\partial v}{\partial \theta} + wV' + \frac{wV}{r} = -\frac{1}{\rho r}\frac{\partial p}{\partial \theta}, \tag{2c}$$

$$\frac{\partial w}{\partial t} + U\frac{\partial w}{\partial x} + \frac{V}{r}\frac{\partial w}{\partial \theta} - \frac{2vV}{r} = -\frac{1}{\rho}\frac{\partial p}{\partial r}. \tag{2d}$$

The density ρ of the fluid in any layer is assumed to be constant, but can take different values in different layers.

To analyze the instability of prescribed flows we employ a normal mode decomposition of the field variables. Since the basic flow state is steady and uniform in the axial and azimuthal directions, we seek a solution of the form

$$p(x,\theta,r,t) = \hat{p}(r)e^{i(kx+m\theta-\omega t)} \tag{3}$$

with similar expressions for the velocity components (u,v,w).

For the jet flows considered, two reductions of the system (2*a-d*) are of interest. First, considering a uniform axial flow velocity U, the modal amplitudes can be expressed in terms of the modal amplitude $\hat{u}(r)$ of the streamwise velocity component using the linearized Euler equations (2*b-c*):

$$\frac{\hat{p}}{\rho} = \frac{\Omega}{k}\hat{u}, \quad \Omega \equiv \omega - Uk - m\frac{V}{r}; \tag{4a}$$

$$\hat{w} = -\frac{i\Omega^2}{k\left(\Omega^2 - \frac{2V}{r}D_*V\right)}\left(\frac{d}{dr} - \frac{m}{r}\frac{D_*V}{\Omega}\right)\hat{u}, \quad D_*V = \frac{1}{r}\frac{d}{dr}(rV); \tag{4b}$$

$$\hat{v} = \frac{m}{rk}\left[1 + \frac{(D_*V)^2}{\Omega^2 - \frac{2V}{r}D_*V}\right]\hat{u} - \frac{1}{k}\frac{\Omega D_*V}{\Omega^2 - \frac{2V}{r}D_*V}\frac{d\hat{u}}{dr}. \tag{4c}$$

Substituting these expressions into the continuity Eq. (2*a*) then yields a single equation for $\hat{u}(r)$. The general form of the equation for arbitrary $V(r)$ is not relevant to our purposes here. Rather, its form in two special cases is used extensively in what follows.

Case A.

$$V = Ar.$$
$$\frac{d^2\hat{u}}{dr^2} + \frac{1}{r}\frac{d\hat{u}}{dr} - \frac{m^2}{r^2}\hat{u} - k^2\left(1 - \frac{4A^2}{\Omega^2}\right)\hat{u} = 0, \tag{5}$$
$$\Omega = \omega - Uk - mA.$$

Case B.

$$V = B/r.$$
$$\frac{d^2\hat{u}}{dr^2} + \frac{1}{r}\frac{d\hat{u}}{dr} - \frac{m^2}{r^2}\hat{u} - k^2\hat{u} = 0, \tag{6}$$
$$\Omega = \omega - Uk - m\frac{B}{r^2}.$$

The general solutions for these special cases can be readily expressed in terms of Bessel functions.

Case A.

$$\hat{u} = C_j J_m(\nu r) + C_y Y_m(\nu r),$$
$$\nu = k\sqrt{1 - \frac{4A^2}{\Omega^2}}. \tag{7}$$

Case B.

$$\hat{u} = C_i I_m(kr) + C_k K_m(kr). \tag{8}$$

In a radially-concentric layer encompassing the polar axis $r = 0$, we require $C_y = C_k = 0$ to avoid singular behavior of the disturbance field on the axis. In the same way, if the radially-concentric layer extends indefinitely in the radial direction, we require $C_i = 0$ so that the disturbance amplitude remains bounded.

For general reference, we note that another simple flow model which allows for shear in the axial velocity field $U(r)$ can be constructed ("simple" here means that analytical expressions for the eigenfunctions can be found). Restricting the swirling flow component to satisfy $D_*V = 0$ and the disturbance field to axisymmetric modes ($m = 0$), the equation for the modal amplitude, now in terms of the radial velocity component, is

$$\frac{d^2\hat{w}}{dr^2} + \frac{1}{r}\frac{d\hat{w}}{dr} - \left\{k^2 + \frac{1}{r^2} + \frac{(rU'' - U')}{r\left(U - \frac{\omega}{k}\right)}\right\}\hat{w} = 0. \tag{9}$$

Relatively simple analytic results are possible for jet core flows $U(r)$ provided the constraint $rU'' - U' = 0$ is satisfied. That is, the axial flow has a parabolic profile of the form $U(r) = U_0 - U_1 r^2$. In this case the eigensolution takes the following form.

Case C.

$$V = \frac{B}{r}, \quad U(r) = U_0 - U_1 r^2.$$
$$\hat{w}(r) = C_1 I_1(kr) + C_2 K_1(kr), \tag{10}$$
$$\Omega = \omega - kU(r).$$

The remaining modal amplitudes are then determined from the relations

$$\frac{\hat{p}}{\rho} = i\left\{\frac{U'}{k} + \frac{\Omega}{k^2}D_*\right\}\hat{w}, \quad \hat{u} = \frac{i}{k}D_*w. \tag{11}$$

The differential operator D_* is defined in Eq. (4*b*). The modal amplitude for the azimuthal velocity perturbation $\hat{v}$ vanishes identically for this class of axisymmetric disturbances. This flow state is known to be neutrally stable

on a linear, inviscid basis provided, of course, that there is no vortex sheet (*i.e.*, jump in axial velocity) at the edge of the jet $r = a$ (cf. Bachelor and Gill, 1962). It is seen here that the same result holds for axisymmetric disturbances when a potential vortex exists along the jet axis.

In constructing a model flow possessing different profiles of axial and azimuthal velocity in concentric layers, interface matching conditions must be imposed to connect the solutions across the boundary separating contiguous layers. For the inviscid instability problem formulated here, the appropriate interface conditions are the continuity of the radial perturbation velocity and the matching of the normal stress (pressure). Supposing the perturbed interface position is defined by $r = r_0 + \eta(x, \theta, t)$, where r_0 is the equilibrium position and $\eta(x, \theta, t)$ denotes the distortion relative to the cylindrical surface $r = r_0$, the linearized kinematic condition, relating the radial velocity perturbation to the interface distortion, is

$$\hat{w} = -i\Omega\hat{\eta} \quad \text{at } r = r_0. \tag{12}$$

The quantity Ω is defined in (4*a*) and $\hat{\eta}$ is a constant amplitude of the modal distortion of the interface defined in the same manner as other dependent variables in the normal mode representation (3). The linearized pressure matching condition is given by the relation

$$\left(\frac{dP}{dr}\bigg|_{r_{0_+}} - \frac{dP}{dr}\bigg|_{r_{0_-}}\right)\hat{\eta} + \hat{p}(r_{0_+}) - \hat{p}(r_{0_-}) = \frac{\sigma}{r_0^2}(1 - k^2 r_0^2 - m^2)\hat{\eta}, \tag{13}$$

where σ is the coefficient of surface tension which is nonzero when different immiscible fluids are present on either side of the interface. The first term in (13) accounts for the perturbed pressure field arising from the distortion of the mean pressure field when the interface position is disturbed from its equilibrium position. The values of the base state radial pressure gradient are determined by the respective swirl velocities and fluid densities through (1).

3. Dispersion relations for model flows

The results presented in the previous section are now applied to several models of swirling flows. These models are constructed by selecting different radially-symmetric mean flow states in two or more concentric layers. In all cases we allow for a uniform axial velocity U_∞ in the outermost layer. Since all the mean flow states represent a parallel flow (*i.e.*, with no spatial development in the axial direction), the uniform ambient streaming flow U_∞ can be readily removed by a Galilean transformation. However, and this is an important point relative to our objectives, we specifically choose not to suppress U_∞ so that a fixed laboratory frame is always implied. In this way the distinction between absolute or convective instability is unambiguously made in reference to this laboratory frame where the ambient axial flow is U_∞. As a consequence a dimensionless parameter, the velocity ratio, will arise (defined subsequently) which will allow application of computed absolute/convective instability transition boundaries directly to laboratory situations.

3.1. Flow model I

We consider first a jet comprised of the mean flows described in Case A and Case B above. The jet consists of a uniform axial velocity U_c and density ρ_c having radius $r = a$ which is in solid body rotation ($V_c = Ar$). This jet is in a concentric tube of radius $r = b > a$. The flow external to the jet has axial velocity U_∞,

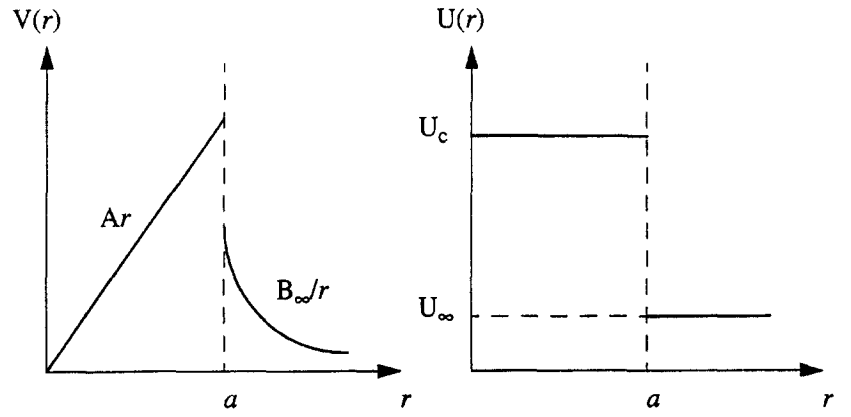

Fig. 1. – Schematic of velocity profiles for Model I.

density ρ_∞, and an irrotational swirling flow defined by $V_\infty = B/r$. A schematic of the velocity profiles for this flow model is given in Figure 1.

It is convenient to define the following dimensionless parameters pertinent to this flow:

$$S = \frac{Aa}{U_c}, \quad R = \frac{U_\infty}{U_c}, \quad q = \frac{\rho_c}{\rho_\infty}, \quad \Delta = \frac{B/a}{Aa}, \quad W_c = \frac{\sigma}{\rho_c U_c^2 a},$$

$$\alpha = ka, \quad d = \frac{b}{a}, \quad \beta = kb = \alpha d, \quad \tilde{\omega} = \frac{\omega a}{U_c}, \tag{14}$$

$$f_c = \tilde{\omega} - \alpha - mS, \quad f_\infty = \tilde{\omega} - R\alpha - mS\Delta, \quad \mu = \nu a = \frac{\alpha}{f_c}(4S^2 - f_c^2)^{\frac{1}{2}}.$$

The principal flow parameters are the swirl ratio S (measuring the peak swirl velocity relative to the axial velocity in the core), the velocity ratio R, the density ratio q, and the (inverse) Weber number W_c. The quantity Δ is a parameter measuring the jump in swirl velocity at the edge of the jet. When $\Delta = 1$ the azimuthal velocity is continuous with the form of a Rankine vortex.

The circumference of the jet is, in general, a vortex sheet possessing both azimuthal and axial vorticity. The velocity ratio R measures the strength of the azimuthal vorticity and the swirl ratio S measures the axial vorticity. Whenever R differs from unity, the Helmholtz instability mechanism is operative leading to the tendency for the vortex sheet to roll up into axisymmetric vortex ring structures. Nonzero values of S, assuming for the moment that $\Delta = 0$ so that swirl is entirely confined within the jet $r < a$, render the flow centrifugally unstable as the circulation drops precipitously across the vortex sheet. The strength of this type of instability will grow as S increases. Values of Δ increasing from zero will decrease the tendency for centrifugal instability leading, as Δ exceeds unity, to a stabilizing of the centrifugal type of instability (at least for axisymmetric $m = 0$ modes). Now, variations of the density ratio q, holding all other control parameters fixed, will affect the growth rate of both the Helmholtz (shear) and centrifugal modes of instability. It is the competition, or interplay, between these modes which is of primary interest in this study, especially as the group velocity of instability waves is affected by the different flow parameters.

Using the parameters defined in (14), the dispersion relation for the model defined in Figure 1 can be written as

$$S^2(\Delta^2 - q) + f_\infty^2 \frac{C_{\alpha\beta(m)}}{D_{2(m)}} - \frac{q(f_c^2 - 4S^2)}{\mu \frac{J'_m(\mu)}{J_m(\mu)} - 2\frac{mS}{f_c}}$$

$$-qW_c(1 - \alpha^2 - m^2) = 0. \tag{15}$$

The second term in this equation is determined from the following combination of modified Bessel functions:

$$C_{\alpha\beta(m)} = \beta\{I_m(\alpha)K'_m(\alpha) - K_m(\alpha)I'_m(\alpha)\},$$
$$D_{2(m)} = \alpha\beta\{I'_m(\alpha)K'_m(\beta) - K'_m(\alpha)I'_m(\beta)\}. \tag{16}$$

We note that, in the limit $d \to \infty$ (*i.e.*, the ambient flow around the jet is of unbounded extent), the ratio $C_{\alpha\beta(m)}/D_{2(m)}$ appearing in (16) reduces simply to the ratio $K_m(\alpha)/\alpha K'_m(\alpha)$.

3.2. Flow model II

Model II consists of a modified version of the columnar vortex sheet model of a swirling jet discussed earlier by Caflisch, Li and Shelly (1993) and by Martin and Meiburg (1994). The base state flow field is comprised of an axisymmetric vortex sheet of radius a, and of infinite length $(-\infty < x < +\infty)$, in which the streamwise velocity jumps discontinuously from its value U_c inside the jet to the value U_∞ in the co-flowing external stream. At the same time, a line vortex with circulation $\Gamma_c = 2\pi B_c$ is positioned on the axis of the jet yielding the swirl velocity distribution B_c/r inside the jet (*i.e.*, for $r < a$). The swirl velocity in the co-flowing stream outside the jet (*i.e.*, for $r > a$) is specified by B_∞/r induced by a line vortex on the jet axis with circulation $\Gamma_\infty = 2\pi B_\infty$. Hence, both a discontinuous jump in azimuthal circulation given by the change in streamwise velocity $\Delta U = U_c - U_\infty$, promoting instability via the Helmholtz mechanism, and a discontinuous jump in streamwise circulation proportional to $\Delta\Gamma = 2\pi(B_c - B_\infty)$, derived from the change in swirl velocity and promoting instability via the centrifugal mechanism when $B_\infty < B_c$, exist at the jet radius $r = a$. At the same time, we suppose that the mass density of the jet fluid ρ_c is different from the ambient density ρ_∞. A schematic of the velocity profiles for this flow model is given in Figure 2.

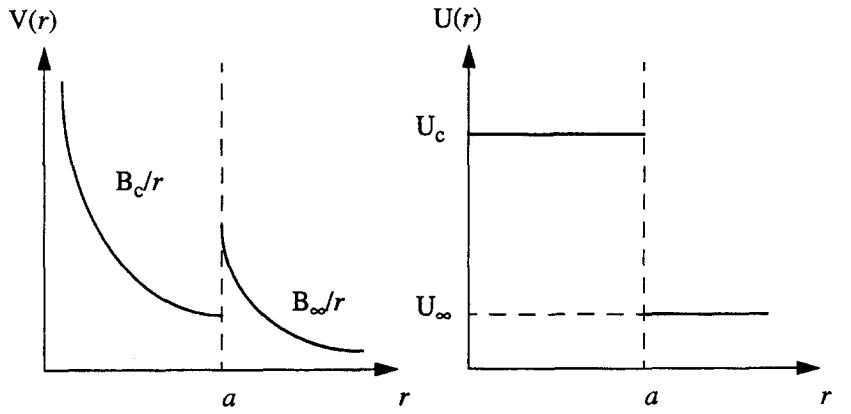

Fig. 2. – Schematic of velocity profiles for Model II.

The relevant dimensionless parameters for this flow are similar to those already defined in (14), except that now the swirl ratio S and the swirl velocity parameter Δ appearing in (14) are replaced by

$$S = \frac{B_c}{aU_c}, \quad \gamma = \frac{B_\infty}{B_c} = \frac{\Gamma_\infty}{\Gamma_c}. \tag{17}$$

The definition of the swirl ratio S compares the swirl velocity at the edge of the jet (*i.e.*, as $r \uparrow a$) with the (uniform) axial velocity of the jet in both cases. In Model I, the maximum swirl velocity occurs at the edge of

the jet and the axial vorticity of the jet is constant across the entire jet $0 < r < a$. In Model II, the axial vorticity is concentrated on the jet axis and the swirl velocity decreases continuously from the jet axis to the edge of the jet $r = a-$. Hence, Model I and II provide a basis for analyzing the effect of the size of the vortical core of the swirling flow, in two extreme limits, on the susceptibility of the flow to appearance of absolute instability.

The dispersion relation for flow described by Model II, shown schematically in Figure 2, is given by the relation

$$S^2(\gamma^2 - q) + \tilde{f}_\infty^2 \frac{K_m(\alpha)}{\alpha K_m'(\alpha)} - q\tilde{f}_c^2 \frac{I_m(\alpha)}{\alpha I_m'(\alpha)} - qW_c(1 - \alpha^2 - m^2) = 0. \tag{18}$$

The dimensionless frequencies $\tilde{f}_\infty$ and $\tilde{f}_c$ have the definitions

$$\tilde{f}_c = \tilde{\omega} - \alpha - mS, \quad \tilde{f}_\infty = \tilde{\omega} - R\alpha - mS\gamma. \tag{19}$$

All other variables are defined in the same way as specified by the relations in (14). It is worth noting here that the eigenfunction $\hat{v}(r)$ for the azimuthal velocity disturbance does not decay to zero in the limit $r \downarrow 0$ for helical modes $|m| = 1$. However, since it approaches a finite constant at $r = 0$, and the base swirl flow becomes unbounded as $r \downarrow 0$, we believe results computed using the linear dispersion relation (18) should still be representative of helical modes with $|m| = 1$ in a swirling jet with a vortical core that is small compared to the jet diameter.

The swirl velocity distributions in these models represent the two simplest, first-order models of a variable density swirling jet and might be expected to yield reasonable representations for instability waves in realistic jet flows when the waves are long relative to the scale of the jet column. The simplicity of these configurations, consisting of two concentric regions of an incompressible fluid separated by a single vortex sheet, is manifested further in that analytic expressions for the dispersion relation can be obtained in each case.

In the present study the dispersion relations (15) and (18) for the two flow models are considered as a relation between the complex frequency $\tilde{\omega}$ and the complex wavenumber α. As such, a search is made to locate the branch point singularities $\tilde{\omega}_0$ in the frequency plane which, through the dispersion relation, is associated with a saddle point α_0 in the wavenumber plane. The pair $(\tilde{\omega}_0, \alpha_0)$ correspond to solutions of the dispersion relation where the group velocity vanishes and are specified by the relation

$$\left.\frac{\partial \tilde{\omega}}{\partial \alpha}\right|_{\alpha_0} = 0. \tag{20}$$

An important quantity related to the determination of the nature of the instability within the bandwidth of unstable waves is the absolute growth rate defined by $\tilde{\omega}_{0i} = \mathrm{Im}\tilde{\omega}_0 = \mathrm{Im}\tilde{\omega}(\alpha_0)$. Whenever $\tilde{\omega}_{0i} < 0$, the instability is of convective type. When $\tilde{\omega}_{0i} > 0$, the instability is of absolute type.

In what follows, results of a numerical study are presented for the transition boundary between absolute and convective instability for various mode numbers m in the space of the flow parameters defined in (14) and (17). These boundaries, and especially their trends with the parameters defining the base flow state in each model, should serve as useful guides in determining conditions where a change in character of jet dynamics can be expected.

The results obtained for the transition boundary between absolute and convective instability for a given set of flow parameters are computed by locating the dominant saddle point of the dispersion relation in the complex α-plane. Images of straight lines $\tilde{\omega}_i$ = constant in the complex $\tilde{\omega}$-plane are mapped to the α-plane and the saddle point with the largest value of $\tilde{\omega}_{0i}$ is identified. An example of this mapping calculation is shown in Figure 3

for an unbounded top-hat jet profile without swirl described either by dispersion relation (15) or (18) with $m = q = R = S = 0$. The result shown in Figure 3 agrees with the earlier calculation by Monkewitz and Sohn (1988). Surface tension effects have been included in the derivation of each of the dispersion relations studied here. Although no specific trends obtained by varying the Weber number are presented, the high-wavenumber cutoff imposed by surface tension on the band of unstable waves provides a useful check on numerical results of the branch point calculation in vortex sheet models.

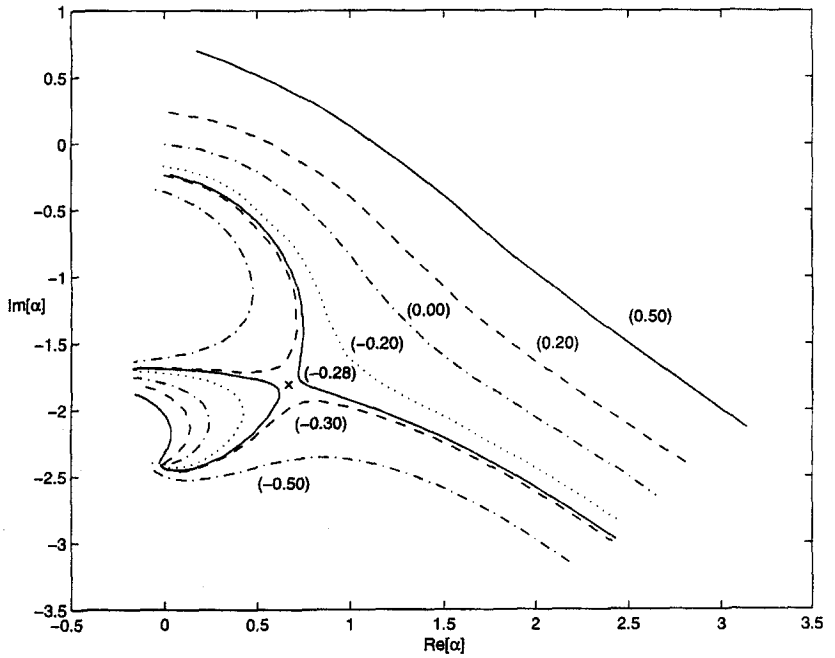

Fig. 3. – The saddle point in the α-plane for flow conditions $m = R = S = 0$, $q = 1$.

4. Results for flow Model I

In this section we present instability characteristics implicit in the dispersion relation (15) describing linear disturbances in a swirl flow where the azimuthal motion is given by uniform axial vorticity in the jet (*i.e.*, solid body rotation). Loiseleux *et al.* (1997) present extensive results for the flow with $q = \Delta = 1$. The results presented here will focus primarily on the effect of varying both q, the density ratio, and Δ, measuring the jump in azimuthal velocity at the circumference of the jet.

To illustrate the role of these parameters analytically we consider two limiting cases of (15). First, consider the limit where $0 < \alpha \ll 1$, $\beta = O(1)$ and $W_c = 0$ for axisymmetric modes ($m = 0$). The leading approximation of the dispersion relation (15) in this limit is

$$J_0(\mu) = \frac{1}{4}\left(\frac{\Delta^2}{q} - 1\right)\mu J_1(\mu) \tag{21}$$

The effect of the swirl parameter S is contained in the variable μ. For the special case when $\Delta = q = 1$, this approximation reduces simply to $J_0(\mu) = 0$ yielding the approximate dispersion relation

$$\tilde{\omega} = \alpha + \frac{2S\alpha}{j_{0,n}}, \tag{22}$$

where the $j_{0,n}$ are the zeros of the Bessel function $J_0(z)$. The point to be emphasized here is that both Δ and q, independently, significantly alter the dispersion relation and they can be expected to play a pivotal role in determining the sign of the group velocity of unstable waves. Of course, the flow is entirely stable in this approximation. A second limit case we consider has $\alpha \gg 1$ and $\beta \uparrow \infty$. In this limit we deduce the following expression for the dimensionless phase speed $c = \tilde{\omega}/\alpha$:

$$\begin{aligned} c = R + \frac{q}{1+q}(1-R)\left\{1 - \frac{3}{16(1+q)}\frac{1}{\alpha} + \cdots\right\} \pm i\frac{\sqrt{q}(1-R)}{1+q} \\ \times \left\{1 - \left[\frac{3}{32}\frac{1-q}{1+q} + S^2\frac{1+q}{2q}\frac{\Delta^2 - q}{(1-R)^2}\right]\frac{1}{\alpha} + \cdots\right\}. \end{aligned} \tag{23}$$

This limiting case reveals that swirl (both S and Δ) affects the first correction to the growth rate, but the density ratio exerts a zeroeth-order influence. The limit described here yields, at leading order, the well-known result for a vortex sheet. In fact, writing the leading order terms on the right-hand side in dimensional form gives familiar expression

$$c = \frac{\rho_\infty U_\infty + \rho_c U_c}{(\rho_\infty + \rho_c)U_c} \pm i\frac{\sqrt{\rho_\infty \rho_c}}{\rho_\infty + \rho_c}\frac{U_c - U_\infty}{U_c}. \tag{24}$$

The roles of the density and velocity ratio are prominently apparent in the result given either in (23) or (24).

Before discussing instability characteristics for flows with different configurations of swirl, we present calculations of the transition boundary between absolute and convective instability for a circular, nonswirling jet flow in an unbounded domain. The boundaries for different modes in the velocity-density ratio space are shown in Figure 4. The instability is of absolute type in the space to the left of a given boundary curve. The result for axisymmetric disturbances ($m = 0$) is in agreement with results already reported by Monkewitz and Sohn (1988). They used the same vortex sheet model to first demonstrate that heating of the jet promotes onset of absolute instability. The axisymmetric mode is found to become absolutely unstable for a jet issuing into a stationary ambient state ($R = 0$) when the density ratio is reduced to a value of about $q = 0.66$. Experiments by Sreenivasan *et al.* (1989) and Monkewitz *et al.* (1990) confirm that the critical density ratio predicted by this simple model describes the transition between the types of instability quite accurately. These experiments also show that dramatic changes in jet structure occur when the jet is absolutely unstable (*i.e.*, that transition to a global dynamics occurs). Figure 4 reveals that helical modes are always more convectively unstable than the axisymmetric mode, but the helical modes can also become absolutely unstable without any counterflow of the ambient stream at lower density ratios.

Using the results for a non-swirling jet flow as a reference, the effect of the swirl parameters S and Δ on the values of $(\tilde{\omega}_0, \alpha_0)$ were evaluated. Some sample results are given in Figures 5 and 6. Figure 5 depicts the variation of the absolute frequency with swirl ratio over a range of density ratios for the axisymmetric mode in a Rankine-vortex jet (*i.e.*, with $m = R = 0$, $\Delta = 1.0$). The addition of swirl in this flow configuration suppresses the tendency for absolute instability. When the swirl ratio increases above about $S = 0.53$, the Rankine-vortex jet is convectively unstable at all density ratios. The same trend is evident in Figure 6, except

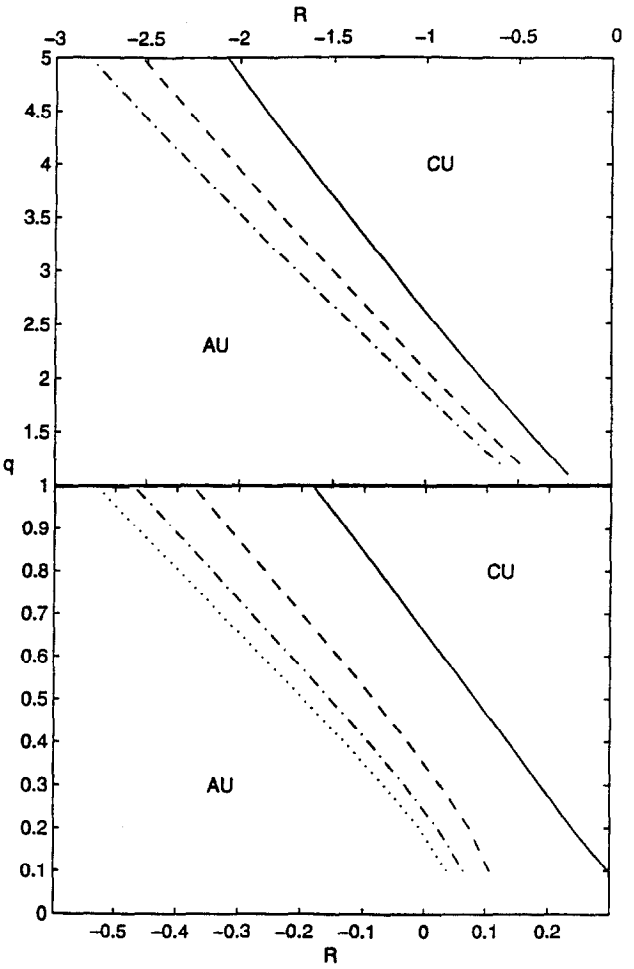

Fig. 4. – The absolute-convective transition boundary for various modes in a non-swirling jet. (—) $m = 0$; (- - - -) $m = 1$; (– · – · –) $m = 2$; (····) $m = 3$.

here we depict the variation of $\tilde{\omega}_{0i}$ and α_{0r} with swirl ratio for a constant density flow. One observes from this figure that retrograde helical modes are likely to become absolutely unstable before their prograde counterparts. Since Loiseleux *et al.* (1997) give extensive results for helical modes in the uniform density Rankine-vortex jet, subsequent results presented here will primarily elucidate the role of swirl and density effects on the axisymmetric mode in jets with different swirl profiles.

In most applications involving swirling jet flows, the circulation outside the jet vanishes. Hence, we study swirling jet flows ranging from the Rankine-vortex jet (*i.e.*, with $\Delta = 1.0$) to a jet with uniform axial vorticity issuing into a non-swirling ambient (*i.e.*, with $\Delta = 0$). The variation of the absolute instability parameters $\tilde{\omega}_{0i}$ and α_{0r} with swirl ratio S for several values of Δ in a jet with $m = R = 0$, $q = 1$ are shown in Figure 7. One observes immediately that the presence of swirl in the ambient flow has a pronounced effect rendering the flow more convectively unstable as Δ increases. According to Rayleigh's criterion (cf. Drazin and Reid, 1981), values of Δ in the range $\Delta < 1$ enhance the centrifugal instability of the vortex sheet. In the Rankine-vortex jet with $\Delta = 1$, the circulation increases monotonically from the jet axis to the outer edge of the jet and then remains constant throughout the ambient region. When $\Delta < 1$ the circulation decreases abruptly at the edge of the jet, with the maximum jump occurring when $\Delta = 0$.

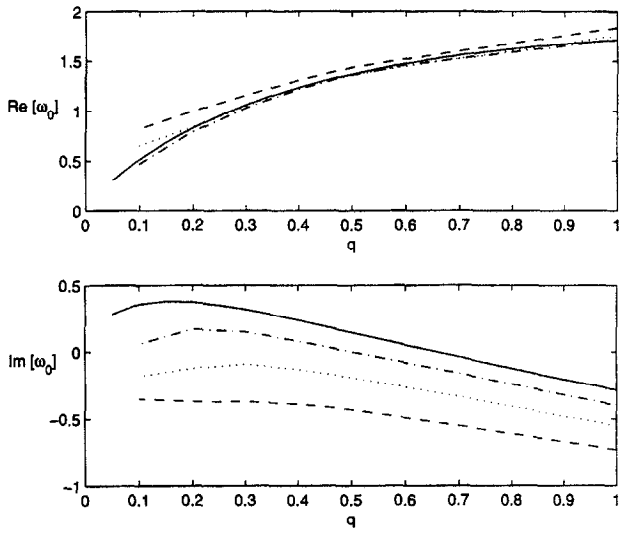

Fig. 5. – Variation of the absolute frequency with swirl ratio and density ratio for Model I with $m = R = 0, \Delta = 1$. (—) $S = 0$; (– · – · –) $S = 0.4$; (····) $S = 0.6$; (- - - -) $S = 0.8$.

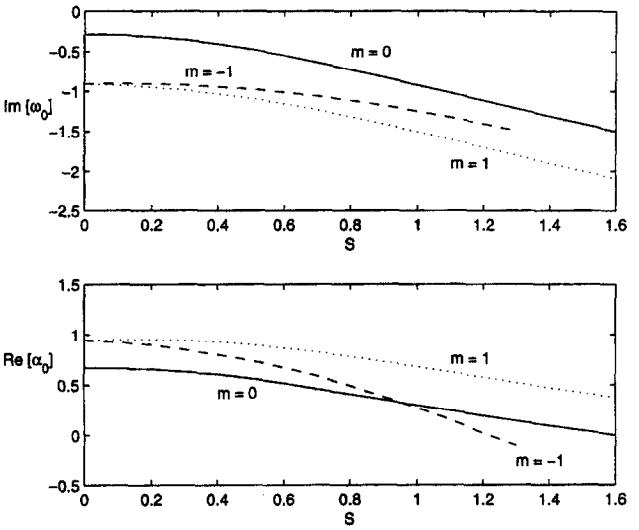

Fig. 6. – Variation of $\tilde{\omega}_{0i}$ and α_{0r} with swirl ratio for different helical modes for Model I, with $R = 0, q = \Delta = 1$.

Some of the results shown in Figure 7 require further comment. The reader will note that an asterisk appears along the curves for fixed values of Δ and that the curve for $\Delta = 0$ is shown dotted past the marked point occurring at a value of the swirl ratio around $S = 2.12$. In tracking the trajectory of the dominant saddle point in the complex α-plane as S is increased, holding all other parameters fixed, the saddle point α_0 moves continuously to decreasing values of α_{0r}. When S reaches the value marked by the asterisk the saddle point lies on the imaginary axis (*i.e.*, $\alpha_{0r} = 0$). For larger values of S the saddle point moves into the left-half of the complex α-plane. The trajectories of the real and imaginary parts of $\tilde{\omega}_0$ and α_0 are entirely smooth as S passes through the marked value. However, the validity of the pair $(\tilde{\omega}_0, \alpha_0)$ as representing acceptable wave disturbances in the flow is in question. Imposition of the condition of exponential decay of the radial eigenfunctions as $r \to \infty$ shows that $\alpha = 0$ is a branch point and that, at least nominally, computation of

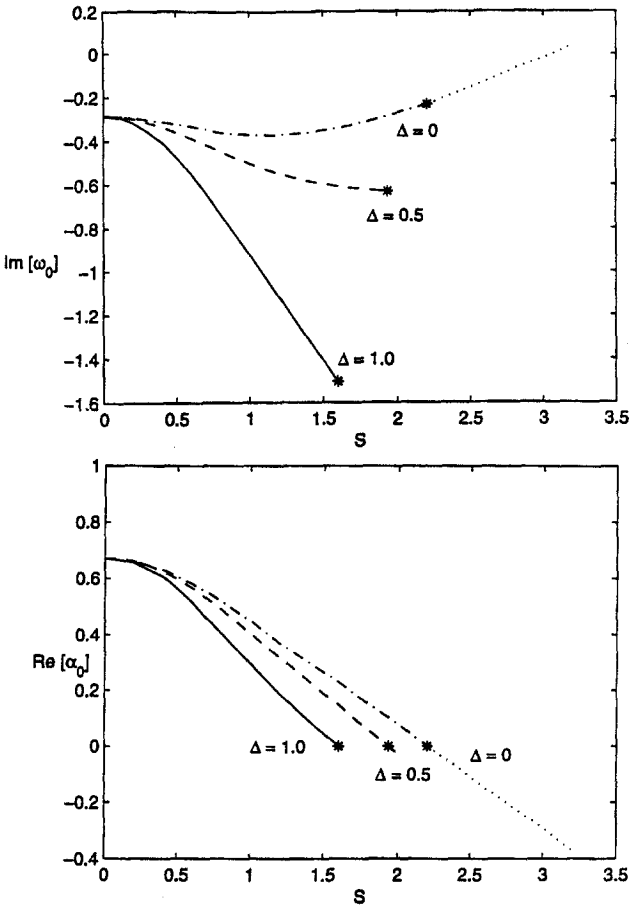

Fig. 7. – Variation of $\tilde{\omega}_{0i}$ and α_{0r} with swirl ratio for different Δ for Model I, with $q = 1$, $m = R = 0$.

the Green's function is restricted to values of α in the right-half plane (cf. Huerre and Monkewitz, 1985). It is counter-intuitive to imagine any abrupt change in propagation characteristics for the wave $(\tilde{\omega}_0, \alpha_0)$ as S increases continuously past the "critical" point. Hence, the implication, and especially the physical significance, of a saddle point associated with the most amplified branch point of the dispersion relation moving into the left-half of the α-plane for physically acceptable flow states requires further examination.

Computations of the absolute frequency $\tilde{\omega}_0$ and α_0 of the type shown in Figure 7 were repeated for a range of density ratios for heated jets. A summary of these calculations appear in Figure 8 and Figure 9. Figure 8 displays the transition boundary for the axisymmetric mode in uniform density, Rankine-vortex jet flows. The required counterflow needed to experience absolute instability increases with increasing swirl ratio. Figure 9 presents transition boundaries between absolute and convective instability for the axisymmetric mode $(m = 0)$ in a flow with $R = 0$ for two swirl profiles. It is seen that the axisymmetric mode in a Rankine-vortex jet is convectively unstable, irrespective of the density ratio, for swirl ratios greater than about $S = 0.53$. On the other hand, the instability type in a jet with solid body rotation throughout its core, and with vanishing swirl or circulation outside, is only slightly influenced by the presence of swirl. As shown in the next section however, the size of the vortical core of the swirling flow plays a very significant role in assessing whether swirling jets are absolutely or convectively unstable. In this case, the swirl profile in the jet core for Model I represents an extreme limit where the vortical core fills the entire jet.

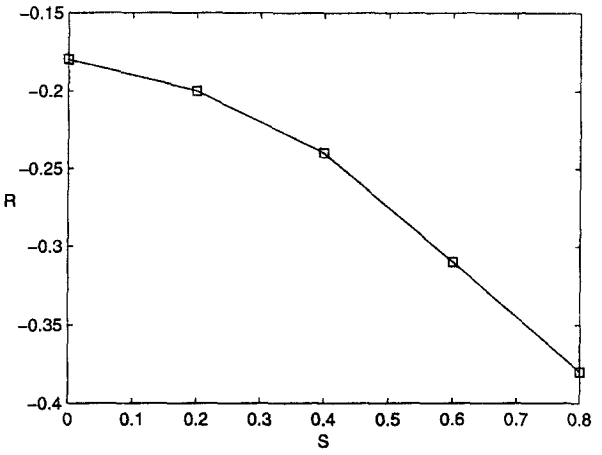

Fig. 8. – The absolute-convective transition boundary for a Rankine-vortex jet ($m = 0$, $q = \Delta = 1$).

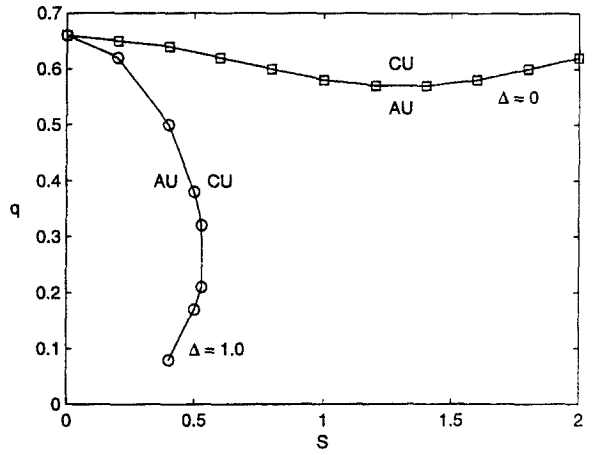

Fig. 9. – Absolute-convective transition boundaries in the q-S plane for Model I with $m = R = 0$.

Since a number of experiments have been performed with swirling flows in a tube, we present some results showing the effect of a concentric, confining boundary enclosing the axial or jet flow. The main results appear in Figure 10 where the absolute growth rate $\tilde{\omega}_{0i}$ is exhibited for several confinement ratios d (cf. Eq. 14). In the absence of swirl, the absolute growth rate is reduced from its asymptotic value by the confinement effect $d < 4$, at least for $q = 1$. It is interesting that increasing values of the swirl ratio can render the confined Rankine-vortex jet more absolutely unstable than its unbounded counterpart. This is evident in the fact that the curves for $d = 3$ and $d = 5$ cross the curve for $d \to \infty$ at different swirl ratios. Since the flow for Model I is, in general, convectively unstable, the effect of confinement was not pursued further.

5. Results for flow Model II

Using the results contained in Figure 4 as a base, instability characteristics for the flow corresponding to Model II and described by the dispersion relation (18) were computed for a range of the relevant parameters. Variations of the absolute frequency $\tilde{\omega}_0$ and absolute wavenumber α_0 with swirl ratio and density ratio for this flow are shown in Figure 11 for heated jets with $m = R = \gamma = 0$. Comparing these results with corresponding

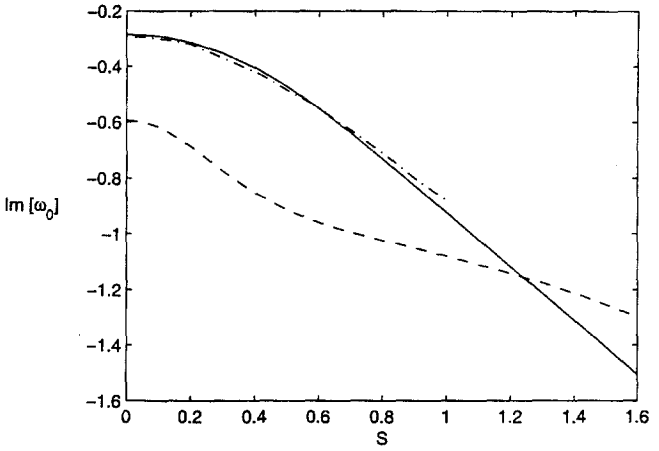

Fig. 10. – Effect of a confining outer boundary on the absolute growth rate of a Rankine-vortex jet ($m = R = 0$, $q = \Delta = 1$). (—) $d \to \infty$: (– · – · –) $d = 5$; (- - -) $d = 3$.

plots for Model I shown in Figure 5, one immediately notices that the effect of swirl on the absolute growth rate is reversed for these two flow models. In Model II where the vorticity is concentrated near the jet-axis, swirl renders the flow more absolutely unstable. When the vorticity is distributed uniformly across the entire jet as in Model I, swirl renders the flow more convectively unstable. These opposing influences of swirl depending on the distribution (or concentration) of the axial-vorticity of the swirling flow comprises one of the most revealing results of this study. In each flow model, however, heating of the jet consistently promotes the onset of absolute instability. Regarding the variation of α_{0r} shown in Figure 11, we note that, even though α_{0r} is tending toward zero as q decreases, under no flow conditions studied did we find the saddle point crossing the imaginary axis, except perhaps, at extremely low values of the density ratio.

Results from a series of calculations like those shown in Figure 11 were used to determine absolute-convective transition boundaries in $q-R-S$ space. Figure 12 gives a summary of these results. We find that a jet exhausting into a stationary ambient state of the same density will exhibit absolute instability for swirl ratios exceeding $S = 0.72$. We find, therefore, that swirling jet flows with concentrated axial-vorticity are likely to become globally unstable as the swirl ratio increases. This change in global character of the flow, rather than any enhanced temporal or spatial growth rate of local instabilities, may be the underlying cause of the measured increase in entrainment rate in some swirling jet flows. It may also underlie the fact that there exists some inconsistency, or at least variation, in the swirl ratios required in different experiments to initiate vortex breakdown in swirling jets. According to the results presented here contrasting two different models, the varying distribution of the axial vorticity across the jet in different experiments will naturally give rise to different breakdown conditions. One also observes from Figure 12 that the *rate of increase* in the critical velocity ratio as the swirl ratio increases is greater for high density ratios than it is for lower density ratios (viz., the divergence of the curves with increasing q). Hence, swirl appears to accentuate the tendency for absolute instability as the density ratio increases, holding all other parameters fixed. This might be explained on the basis that centrifugal forces promoting deformation of the jet boundary become stronger as the jet density is increased relative to the ambient density.

Figure 13 exhibits the effect of mode number and density ratio on the absolute-convective transition boundary. As is already evident from previous results for either flow model, the boundary separating domains of absolute instability (on the left) and convective instability (on the right) are displaced toward negative velocity ratios as the density ratio increases. What is apparent in this figure, at least for the limited range of parameters studied, is that the axisymmetric mode transitions more readily to absolute instability than do the helical modes. Also, and what is in contrast with the results for Model I shown in Figure 6, the prograde mode is observed to

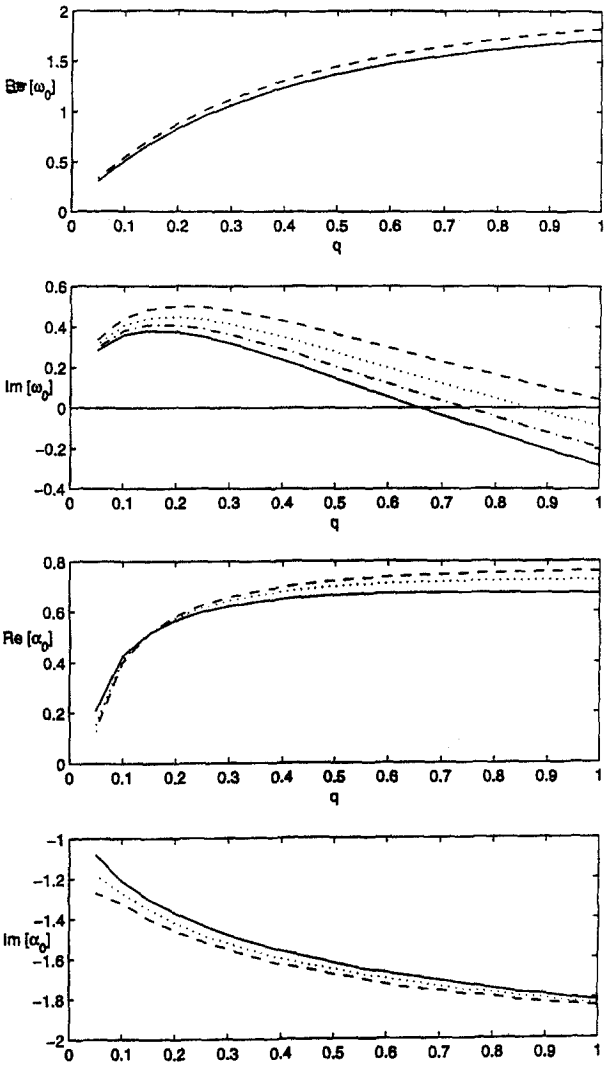

Fig. 11. – Variation of the absolute frequency and wavenumber with swirl ratio and density ratio for Model II with $m = R = \gamma = 0$. (—) $S = 0$; (– · – · –) $S = 0.4$; (····) $S = 0.6$; (- - - -) $S = 0.8$.

be more absolutely unstable than the retrograde mode. This represents another change in tendency when the concentration of the axial vorticity in the jet is varied.

Figures 14 and 15 reveal the effect of the circulation ratio γ on the transition boundary. Figure 14 defines the critical velocity ratio for the axisymmetric mode in a homogeneous jet at a nominal swirl ratio $S = 0.4$. Increasing the circulation ratio causes the jet instability to become progressively more convectively unstable. Increasing the circulation ratio to values $\gamma > 1$ will, by virtue of Rayleigh's criterion for centrifugal instability, stabilize the centrifugal mode of instability. Nevertheless, the shear mode remains unstable and is controlling insofar as the nature of the instability is concerned.

Figure 15 presents the effect in another way, as well as results for the helical mode $m = 1$. When there is no jump in the axial circulation across the vortex sheet (*i.e.*, $\gamma = 1$), the critical velocity ratio for onset of absolute instability is invariant with the swirl ratio. When the jet column is centrifugally unstable ($\gamma < 1$), the critical velocity ratio increases with the swirl ratio; that is, the jet is more absolutely unstable as the swirl ratio increases. When $\gamma > 1$, the jet becomes more convectively unstable. Clearly, the jet is most absolutely unstable when

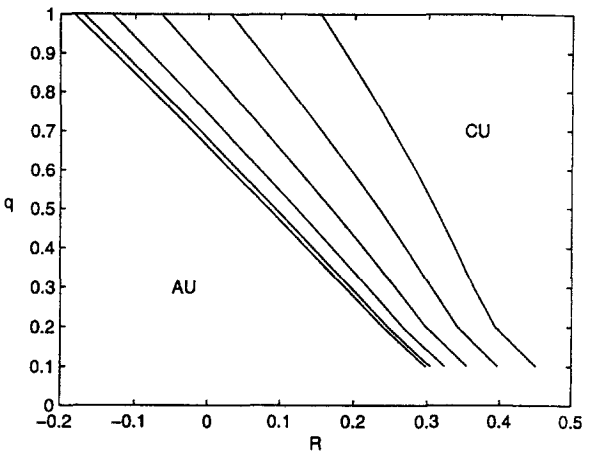

Fig. 12. – Absolute-convective transition boundaries for Model II with $m = \gamma = 0$. The swirl ratio S is constant on each curve, varying by increments of 0.2 and starting from $S = 0$ on the left and ranging to $S = 1.0$ on the right.

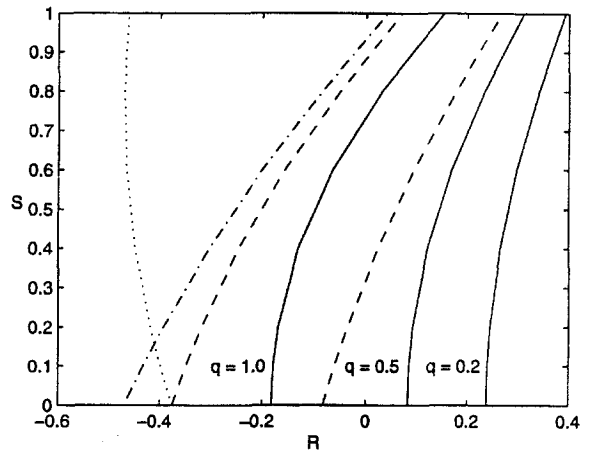

Fig. 13. – Variation of the transition swirl ratio with velocity ratio for selected density ratios and mode numbers when $\gamma = 0$. (—) $m = 0$; (- - - -) $m = 1$; (·····) $m = -1$; (– · – · –) $m = 2$.

the jet is most centrifugally unstable. This suggests that the generation of a swirl flow in the ambient which is oppositely directed from that of the jet might further enhance the susceptibility of a jet to become absolutely unstable to helical modes. Of course, Rayleigh's criterion for centrifugal instability which states that the square of the circulation should decrease with increasing radius for instability of the axisymmetric mode is unaffected by the *sign* of the circulation. We have elected not to explore here other jet configurations that derive from compound jet nozzles, etc. and that involve several contiguous layers possessing different swirl velocity profiles.

Since swirl is found to enhance the onset of absolute instability in jet flows, we decided to explore briefly the tendency, or lack thereof, for absolute instability in swirling wake flows defined by the swirl profile in Model II. Loiseleux *et al.* (1997) present results for uniform density wake flows of the Rankine-vortex type. For our purposes we define the wake velocity and swirl ratios as

$$R_w = \frac{U_c}{U_\infty}, \quad S_w = \frac{B_c}{aU_\infty} = SR_w. \tag{25}$$

The reference velocity for the jet was the core velocity and the velocity ratio R measured the strength of the co-flow $(R > 0)$ or the counter-flow $(R < 0)$ relative to U_c. In a wake flow, the reference velocity is

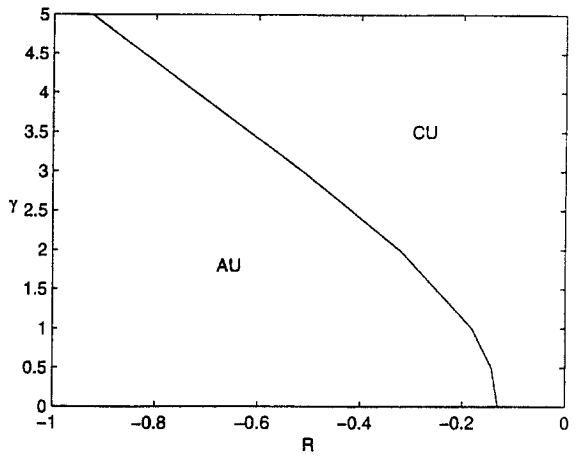

Fig. 14. – The effect of circulation ratio γ on the absolute-convective transition boundary for Model II with $m = 0$, $q = 1$, $S = 0.4$.

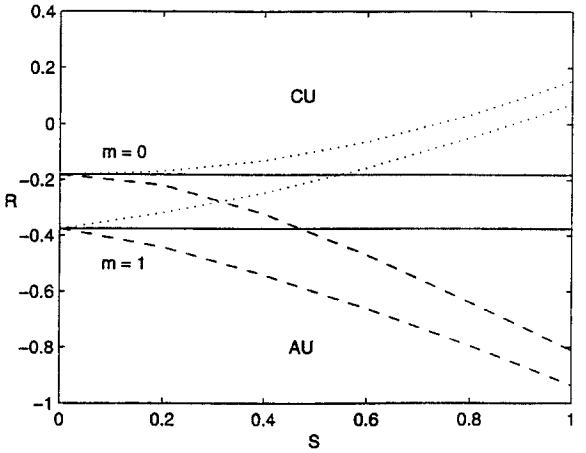

Fig. 15. – Variation of the critical velocity ratio with swirl ratio for selected circulation ratios and mode numbers in a jet with $q = 1$. (· · · · ·) $\gamma = 0$; (—) $\gamma = 1$; (- - - - -) $\gamma = 2$.

the ambient velocity and the strength of the core flow U_c compared with U_∞ is measured in terms of the wake velocity ratio R_w.

Considering the axisymmetric mode in a wake with $R_w = 0$ and $\gamma = 0$ (*i.e.*, no circulation outside the wake), the absolute-convective transition boundary is shown in Figure 16. In contrast to a jet, a cold (high density) wake is more absolutely unstable than a uniform density flow. This opposing effect of density ratio between jets and wakes was noted earlier for plane flows by Yu and Monkewitz (1990). In concordance with the results for a jet with the same swirl profile (cf. Figure 12), swirl renders the wake more absolutely unstable. At a wake swirl ratio of about $S_w = 1.6$ a uniform density wake flow with $R_w = 0$ transitions from convective instability to absolute instability.

The influence of mode number and velocity ratio on this transition boundary is shown in Figure 17 for a uniform density wake flow ($q = 1$). Interestingly, the helical modes of instability are found to be more absolutely unstable than the axisymmetric mode, a result which seems to persist at all swirl ratios. The intercept values of R_w for the different modes at $S_w = 0$ are (–0.43, –0.19, –0.10) for ($m = 0$, $m = \pm 1$, $m = -2$) respectively. Another contrast between jet and wake flows with the Model II swirl profiles is that the retrograde

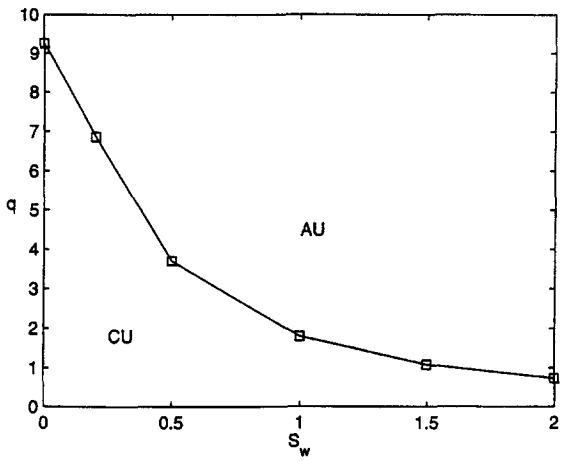

Fig. 16. – The absolute-convective transition boundary for a swirling wake ($m = R = \gamma = 0$).

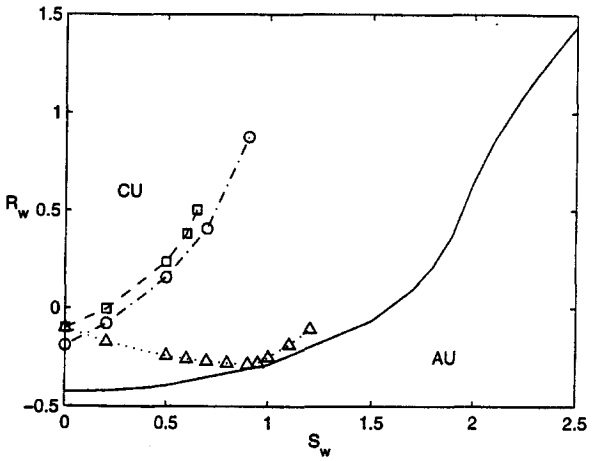

Fig. 17. – The effect of helical mode number on the absolute-convective transition for a wake with $q = 1, \gamma = 0$. (—) $m = 0$; (····) $m = 1$; (– · – · –) $m = -1$; (- - - -) $m = -2$.

helical modes are more absolutely unstable than their prograde counterparts in wakes, with the opposite effect in jets (cf. Figure 13).

6. Concluding remarks

The relation of the onset of absolute instability in a swirling jet to the appearance of vortex breakdown is still an open, but in our minds, quite important issue. Various criteria for vortex breakdown in swirling flows have been proposed, many of which are not entirely unrelated to the idea pursued here that breakdown is related to the transition of local instabilities from convective to absolute type with consequent onset of a global instability. Squire (1956) and Benjamin (1962) advanced the conjecture that breakdown is related to a supercritical-subcritical transition of long waves on the *columnar* swirling flow. Tsai and Widnall (1980) later suggested that incipient breakdown is realized when the flow reaches a state where the group velocity of some isolated band of temporally amplified, linear instability waves vanishes in the laboratory frame. Interesting extensions of these ideas have been advanced recently by Wang and Rusak (1997). They have identified global

bifurcations of the steady, inviscid equations of motion for columnar swirling flows and have related the transition between new steady flow states to the loss of stability of a given state along its branch in the solution parameter space. All of these proposed breakdown mechanisms rely on wave arguments and are essentially inviscid, albeit with some quantitative dependence on the Reynolds number. Also, they all yield a breakdown criterion defined in terms of a swirl number. The essentially inviscid nature of vortex breakdown processes has been argued by Leibovich (1984), while Spall *et al.* (1987) have proposed a critical Rossby number (*i.e.*, inverse swirl ratio in the present notation) condition for appearance of breakdown. They suggest the critical condition $S > S_{\text{crit}} = 1.67 \pm 0.08$ as providing a good correlation of experimental results for a range of swirling flows with uniform density. However, it is our opinion that the satisfactory validation of any given mechanism, and the decisive differentiation between mechanisms, still awaits carefully formulated and designed experimental configurations for either laboratory or numerical study.

The experimental observations of increased spreading rates in jets with increasing swirl ratios seems to be quite well correlated with the appearance of vortex breakdown somewhere in the jet column. As the swirl ratio is increased, the observations by Panda and McLaughlin (1994), for example, show that vortex breakdown moves upstream toward the jet origin. The Model II swirling jet flow studied here yields a critical swirl angle (where $\phi = \tan^{-1}(S)$ for a jet with $R = \gamma = 0$) of $\phi = 36°$ for a uniform density jet issuing into a stationary ambient flow. Such an angle is not atypical for swirl angles leading to vortex breakdown reported, for example, by Hall (1982). Most reports of experimental observations of critical swirl angles associated with vortex breakdown are for swirling flows in ducts, often associated with weakly adverse pressure gradients (see, for example, Leibovich, 1983; and Escudier, 1988). Such effects, including that of finite Reynolds number, are obviously absent in the present calculations. Based on experience with mixing layers, viscous effects delay the onset of absolute instability (e.g., a greater counterflow is required for a mixing layer) and the presence of boundaries confining the flow makes the flow more stable when the confining boundary is on the low-speed side of the mixing layer. Extrapolating these trends, the critical swirl angle can be expected to be slightly higher in any real swirling flow, and especially in a confined flow, than predicted by the highly-idealized flows analyzed here. Of course, if the appearance of vortex breakdown is associated with the onset of global instability, the flow will necessarily be slightly super-absolutely unstable over some finite spatial extent of its development, implying again that the swirl ratio will have to (marginally) exceed that for the critical occurrence of local absolute instability.

The jet flow models studied here are clearly most relevant near the jet exit in the early development region where the shear layers are thin. It would be of considerable interest to examine how the absolute-convective transition boundaries are displaced as the shear layer thickness in the jet is increased at fixed swirl ratio. Such a study would provide valuable information relating to the possible link between the *position* of vortex breakdown in a swirling jet and the onset of absolute instability, or even a global instability. It is worth noting that a study of the absolute/convective instability characteristics of the Batchelor vortex model, which has continuously differentiable profiles of axial and swirl velocity, performed by Delbande *et al.* (1997) shows that swirl enhances the tendency toward absolute instability, reducing the required counterflow in a jet for the onset of absolute instability from $0.64U_c$ to $0.015U_c$. Velocity profiles of the Batchelor vortex jet are more relevant to a fully-developed flow where the size of the vortical core is commensurate with the diameter of the jet.

One of the principal results emerging from this study is the significant role played by the concentration, or distribution, of axial vorticity of the swirling flow in determining the conditions for absolute instability. The more concentrated the vortical core of the swirling flow compared to the jet diameter, the greater the tendency toward absolute instability. No account of this effect has been made in the correlation made by Spall *et al.* (1987) in obtaining a critical swirl ratio for onset of breakdown. Our results clearly suggest that an additional length scale parameter should be evident; at least if the proposed idea that vortex breakdown is related to the onset of a global

instability is valid. This length-scale effect has immediate application to the design of nozzles used to produce a swirling flow, and can be exploited to advantage if the use of swirl is intended to promote or enhance mixing.

Acknowledgements. – This work was supported in part by AFOSR under Contract No. F49620-94-1-0358.

REFERENCES

BATCHELOR G. K. and GILL A. E., 1962, Analysis of the stability of axisymmetric jets, *J. Fluid Mechs.* **14**, 529-551.

BENJAMIN T. B., 1962, Theory of the vortex breakdown phenomenon, *J. Fluid Mech.*, **14**, 593-629.

BILLANT P., CHOMAZ J.-M. and HUERRE P., 1997, Experimental study of vortex breakdown in swirling jets, Submitted to *J. Fluid Mech.*

CAFLISCH R. E., LI X. and SHELLY M. J., 1993, The collapse of an axisymmetric swirling vortex sheet, *Nonlinearity*, **6**, 843-000.

CHOMAZ J.-M., HUERRE P. and REDEKOPP L. G., 1988, Bifurcations to local and global modes in spatially developing flows, *Phys. Rev. Lett.*, **60**, 25-28.

CHOMAZ J.-M., HUERRE P. and REDEKOPP L. G., 1991, A frequency selection criteria in spatially developing flows, *Stud. Appl. Math.*, **84**, 199-144.

DELBANDE I., CHOMAZ J.-M. and HUERRE P., 1997, Absolute/convective instabilities in the Batchelor vortex: a numerical study of the linear impluse response, Submitted to *J. Fluid Mech.*

DRAZIN P. G. and REID W. H., 1981, *Hydrodynamic Stability* (Cambridge University Press, Cambridge).

ESCUDIER M. P., 1988, Vortex breakdown: observations and explanations, *Prog. Aerospace Sci.*, **25**, 189-229.

HALL M., 1972, Vortex breakdown, *Ann. Rev. Fluid Mech.*, **4**, 195-218.

HUERRE P. and MONKEWITZ P. A., 1985, Absolute and convective instabilities in free shear layers, *J. Fluid Mech.*, **159**, 151-168.

HUERRE P. and MONKEWITZ P. A., 1990, Local and global instabilities in spatially developing flows, *Ann. Rev. Fluid Mech.*, **22**, 473-537.

LEIBOVICH S., 1983, Vortex stability and breakdown: Survey and extension, *AIAA J.*, **22**, 1192-1206.

LOISELEUX T., CHOMAZ J.-M. and HUERRE P., 1997, The effect of the swirl on jets and wakes: linear instability of the Rankine vortex with axial flow, Accepted for publication in *Phys. Fluids.*

MARTIN J. E. and MEIBURG E., 1994, On the stability of the swirling jet shear layer, *Phys. Fluids*, **6**, 424-426.

MICHALKE A., 1984, Survey on jet instability theory, *Prog. Aerospace Sci.*, **21**, 159-199.

MONKEWITZ P. A. and SOHN K. D., 1988, Absolute instability in hot jets, *AIAA J.*, **26**, 911-916.

MONKEWITZ P. A., BECHERT D. W., BARSIKOW B. and LEHMANN B., 1990, Self-excited oscillations and mixing in a heated round jet, *J. Fluid Mech.*, **213**, 611-639.

PANDA J. and MCLAUGHLIN D. K., 1994, Experiments on the instabilities of a siwrling jet, *Phys. Fuids*, **6**, 263-276.

SPALL R. E., GATSKI T. B. and GROSCH C. E., 1987, A criterion for vortex breakdown, *Phys. Fluids*, **30**, 3434-3440.

SQUIRE H. B., 1956, Rotating Fluids, *Surveys in Mechanics* (eds. Batchelor & Davies), Cambridge University Press.

SREENIVASAN K. R., RAGHU S. and KYLE D., 1989, Absolute instability in variable density round jets, *Expts. in Fluids*, **7**, 309-317.

TSAI C.-Y. and WIDNALL S. E., 1980, Examination of group-velocity criterion for breakdown of vortex flow in a divergent duct, *Phys. Fluids*, **23**, 864-870.

WANG S. and RUSAK Z., 1997, The dynamics of a swirling flow in a pipe and transition to axisymmetric vortex breakdown, *J. Fluid Mech.*, **340**, 177-223.

YU M.-H. and MONKEWITZ P. A., 1990, The effect of nonuniform density on the absolute instability of two-dimensional inertial jets and wakes, *Phys. Fluids A*, **2**, 1175-1181.

(Manuscript received March 7, 1997;
revised November 12, 1997.)